RAMAN STRUCTURAL AND GAMMA RADIATION SHIELDING FEATURES FOR AMORPHOUS MATERIALS: TLBLa(Nb/Ti)

H. ALMOHIY[a], M. SAAD[a,b], E. R. SHAABAN[c], Y. M. ABOU DEIF[d],
M. REBEN[e], E. YOUSEF[d,*]
[a]*Radiological Science Department – Faculty of Applied Medical Science – King Khalid University, P. O. Box 9004, Abha, Saudi Arabia.*
[b]*Physics Department- Faculty of science –Mnasoura University, Egypt.*
[c]*Physics Department, Faculty of Science, Al-Azhar University, Assuit, 71542, Egypt*
[d]*Physics Dep., Faculty of Science, King Khalid University, P. O. Box 9004, Abha, Saudi Arabia.*
[e]*Faculty of Materials Science and Ceramics, AGH – University of Science and Technology, al. Mickiewicza 30, 30-059 Cracow, Poland*

The gamma radiation protection parameter for the TeO_2-$LINbO_3$-BaF_2-La_2O_3 network modified by Nb_2O_5/TiO_2 in the present work. The following compounds have been examined: [$77.53TeO_2$-$7.31LiNbO_3$-$4.16Nb_2O_5$-10% BaF_2-$1.0La_2O_3$, sample code TSH1), [$71.69TeO_2$-$7.31LiNbO_3$-$10BaF_2$-$1.0La_2O_3$, sample TSH2] and [$76.69TeO_2$-$7.31LiNbO_3$-$5TiO_2$-$10BaF_2$-1% La_2O_3 and sample code TSH3]. Within this, we specify the criteria for shielding such as mass attenuation coefficients (μ_m/ρ), effective atomic numbers (Z_{eff}), electron density (Ne), half-value layers (HVL), mean free path (MFP). The TSH3 glasses have a greater gamma-ray safety performance because of a higher value of HVL, ($\mu m/\rho$), and MFP. The observed glasses display good gamma ray safety compared to used standard radiation-shielding materials, namely RS-360, and RS-520. Finally, the structure of these glasses investigates at wavenumber in the range 50 to 1200 cm-1 by using Raman spectra.

1. Introduction

This is important to note that as insulation protection for gamma radiation, different opaque materials such as concrete have been suggested. Long time exposure to heavy radiation such as gamma rays causes cancers and mortality that induces genetic anomalies. Recently, glasses have the greatest ability to be utilized in diagnostic imaging centers, X-ray rooms and CT scans, scintillation, radiation therapy chambers, and laboratory studies as innovative radiation detection techniques. This generated international interest in studying such doping glasses of heavy metal oxide (HMO) for different uses for X-ray, gamma-ray, and neutron shielding. HMO glasses have concentrated mainly on radiation safety, since these glasses have properties that meet both radiation shielding requirements and low cost and light sensitivity of such glasses, offering interesting advantages in different applications. In terms of radiation protection, heavy glasses have attracted further attention because such glasses have properties that satisfy both radiation shielding criteria as well as low cost and light sensitivity [21– 23]. Suitable products for these applications must have some key specifications such as easy, lightweight, environmentally friendly manufacturing and strong radiation shielding ability (e.g. low MFP and strong Zeff). Several authors have reported beforehand the shielding properties of glasses for radiation shielding suitability of developed tellurite glasses [14]. A detailed study of the mechanical, elastic, and shielding properties of lead zinc phosphate glasses, tellurite, and bismuth-modified zinc

borotellurite glass shielding properties. Kaky et al. [24] reported that the tellurite alumina glasses with composition $TeO_2- B_2O_3-ZnO- Li_2O-Al_2O_3-MgO$, can be used as shielding gamma ray protect. Sayyed et al [25] reported some highly dense transparent glasses within $B_2O_3-WO_3-BaO-Na_2O-PbO$ system, they, found that the heavy density of the PbO improves the radiation shielding ability for application. Kurudirek et. al. [26] studied glass in the composition of $Bi_2O_3 - 10Li_2O - (80 - x) B_2O_3$ where x = 10 − 50 mol%, they concluded that the best glass sample for radiation protection at Bi_2O_3 content of 50 mol% with a density (ρ= 7.082 g/cm^3). From the above, we investigate the structural and shielding radiation such as; HVL, $(\frac{\mu_m}{\rho})$, MFP, and Z_{eff} of prepared glasses. This study will be useful in creating new materials in gamma-ray shielding applications.

2. Materials and theory

The process of prepared glasses with composition of [77.53TeO$_2$- 7.31LiNbO$_3$- 4.16Nb$_2$O$_5$- 10BaF$_2$- 1.0La$_2$O$_3$, (sample code TSH1)], [71.69TeO$_2$- 7.31LiNbO$_3$- 10Nb$_2$O$_5$- 10La$_2$O$_3$, (sample code TSH2) and [76.69TeO$_2$- 7.31LiNbO$_3$- 5TiO$_2$- 10BaF$_2$- 1.0La$_2$O$_3$, (sample code TSH3)) were reported in Ref. [27] and Table (1).The nominal composition of metal oxides in (mol%), densities (ρ), weight fraction of elements (*wt.*) and samples codes of prepared glasses are summerizied in Table (1, 2). The $\left(\frac{\mu_m}{\rho}\right)$ values for prepared glasses can be evaluated by the relation as; $\left(\frac{\mu_m}{\rho}\right) = \sum_i w_i \left(\mu_m/\rho\right)_i$; where w$_i$ and (μ_m/ρ)$_i$ represent the fractional weight and mass attenuation coefficient of the ith constituent in the mixture, respectively [27, 28], which is computed by using the WinXCom program [29]. Moreover, we calculated the mean free path ($MFP= 1/\mu_m$) (in cm), which is defined by the distance traveled between two gamma-ray collisions, it depends on the energy of gamma-ray and on the type of the shielding material [30- 32]. The half value thickness HVL, which is the thickness needed from material to decease the intensity to half its initial value, is calculated by the relation as follows; $HVL = ln(2)/\mu_m$ [30-33].

Table 1.   Glasses composition in mol% and density, ρ, in (g/cm^3) [27].

Samples	TeO$_2$	LiNbO$_3$	BaF$_2$	La$_2$O$_3$	Nb$_2$O$_5$	TiO$_2$	ρ
TSH1	77.53	7.31	10	1.0	4.16	0	5.2845
TSH2	71.69	7.31	10	1.0	10	0	5.2278
TSH3	76.69	7.31	0	1.0	0	5	5.2858

Table 2. The weight fraction of elements in the percentage of the prepared glass samples.

Samples	Te	Li	Nb	Ba	F	La	Ti	O
TSH1	0.594539	0.003049	0.087273	0.082533	0.022837	0.016696	0	0.193073
TSH2	0.529996	0.002939	0.147010	0.079566	0.22016	0.016096	0	0.202375
TSH3	0.619385	0.003211	0.042988	0.086923	0.024052	0.017585	0.1515	0.190706

The Z_{eff} signifies partial photon interactions with the shielding material. The Z_{eff} can be directly calculated by using the relation below [30, 34]:

$$\left(Z_{eff}\right) = \sum_i f_i A_i (\mu/\rho)_i / \sum_j f_j A_j (\mu/\rho)_j \tag{1}$$

where f$_i$ refers to the fractional abundance, and A$_i$ is the atomic weight. The Z_{eff} is related to another parameter known as the electron density (N$_{eff}$) by the next formula [35]:

$$\left(N_{eff}\right) = N_A\, n\, Z_{eff}\, /\, \sum_i n_i\, A_i \quad (electrons/g) \tag{2}$$

Here, n_i is the total number of atoms in the glass sample.

3. Results and discussion

Fig. 1 shows the values of the (μ_m/ρ) linear mass attenuation coefficient around the energy spectrum of 0.03-3 MeV. It will note that at first energy the attenuation factor, namely $\mu m/\pi$, is very high and decreases rapidly with the change in energy value. Photoelectric phenomenon as discussed early by Waly et al.[36] can be due to the comparatively small values in the attenuation factor at 15 keV. Fig. 1 depicts the values of linear mass attenuation attributed to the partial photon interactions as well as the influence of Compton scattering with the shielding material in various energy regions, The ratio of (μ_m/ρ) to the chemical composition of the present glass corresponds to the possibility that the gamma-rays induce further attenuation in TSH3 (see Fig. 1), which has a higher weight fraction of Te=0.619 (i.e., glassesTSH3 are greater than those of TSH1 and TSH2, see Table 2). The present glass studied by the shielding parameter (Zeff) which helps in the nuclear shielding industry to provide conclusive details for its operation. Calculation of this parameter by using the Eq. 1. The findings of Z_{eff}, for TSH1, TSH2 and TSH3 glasses are listed at varying gamma photon energy (Table 3).
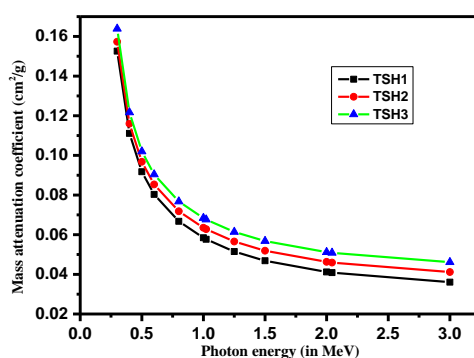
Fig. 1. Mass attenuation coefficient (μ_m/ρ) of prepared glasses.

Table 3. The effective atomic number(Z_{eff}) and The values of effective electron density, Ne of the prepared glass samples at different γ-ray photon energies.

Samples Code	The effective atomic number (Z_{eff})				The values of effective electron density, Ne x 10^{23} (electron/g)			
	0.356 MeV	0.662 MeV	1.173 MeV	1.33 MeV	0.356 MeV	0.662 MeV	1.173 MeV	1.33 MeV
TSH1	25.85	21.949	21.707	22.037	3.2154	2.7301	2.7	2.7411
TSH2	21.797	22.679	22.706	22.653	2.6297	2.7361	2.7394	2.7329
TSH3	26.684	22.545	22.289	22.637	3.2173	2.7183	2.6873	2.7293

The active atomic number of composite glass is observed to improve with an improvement in the mass fraction of Tellurium (Te), which is also apparent attributed to its higher atomic number relative to other constituents present. The increase in Z_{eff} and an improvement in the amount of tellurium indicates that with the incorporation of TeO_2 the shielding potential of the glasses is improved. It is observed that Z_{eff} initially reduces on the low side of the gamma-ray intensity and remains relatively steady. Zeff values over ~900 keV are attributed to the influence

of the incoherent scattering mechanism (Compton) whose cross-section is proportional to the Z. This can be shown in Table 3, the dependencies of Z_{eff} and N_{eff} quantities on photon energy are nearly identical to one another for the present glasses. According to this result, for the chosen glass structure, TeBTi6 has excellent photon attenuation competence, and the amount of Bi_2O_3 is needed to improve the attenuation ability. It should be remembered that the lowest Zeff for TeBTi1 and TeBTi6 glasses exist at 1.5 MeV and equals 22.53, 23.24, 23.93, 24.60, 25.25 and 25.89 respectively [37]. Similarly, N_{eff} has large values in the present glasses at a minimum (E < 0.1 MeV), which decreases the concentration of more electrons at lower energy levels per unit of mass. Although the lowest Neff was found in the intermediate energies, this is due to the Compton scattering dominance. A certain absorber or target's photon shielding efficiency may be calculated by large amounts of MFP or HVL. The fewer the MFP and HVL rates, the more the effective absorber can that the more photons, from the blinding point of view. Table 4 obtained the test MFP and HVL for TSH1 to TSH3 glasses at photon energy varying from 0.356 to 1.33 MeV. Significant quantities of MFP or HVL may be measured for a specific photon shielding absorber or desired performance.

Table 4. Half value layer (HVL) and Mean free path (MFP) of the prepared glass samples at different γ-ray photon energies.

Samples Code	Half value layer (HVL) (cm)				Mean free path (MFP) (cm)			
	0.356 MeV	0.662 MeV	1.173 MeV	1.33 MeV	0.356 MeV	0.662 MeV	1.173 MeV	1.33 MeV
TSH1	1.0112	1.8249	2.4436	2.534	1.4589	2.6266	3.5368	3.6541
TSH2	1.0356	1.8541	2.468	2.571	1.41	2.6316	3.512	3.6264
TSH3	0.974	1.8069	2.4136	2.5136	1.4905	2.6721	3.5577	3.6614

Throughout the blinding viewpoint, the lower the MFP and HVL concentrations, the more effective the absorber could be. Table 4 displays TSH1 to TSH3 glasses of photon energy levels between 0.356 and 1.33 MeV for the MFP and HVL measurements. It indicates that the chosen glasses have a higher radiation shield strength at lower energy. The present glasses were compared to different glass types[38-40] and concrete[39] to photon attenuation capabilities [39]. Relation [38-40] shows the mean free paths of prepared glasses (TSH1, TSH2, TSH3) below LIBTe40 and RS-253-G18 (see Fig. 2).
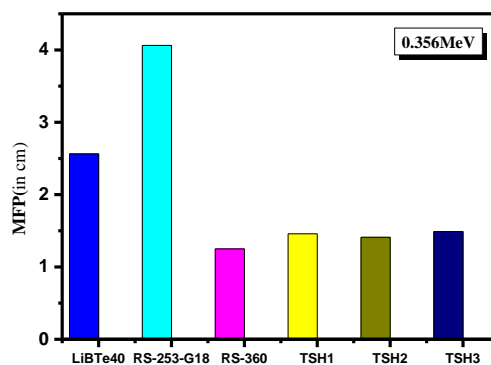
Fig. 2. Mean Free Path (in cm) of LIBTe40, RS-253-G18, RS-360, TSH1, TSH2, and TSH3 glasses.

Otherwise, the MFP values of TSH1, TSH2, TSH3 glasses are nearly the same as those of the ferrite doped concrete, higher than those mentioned in RS-360. It says that the chosen glasses have a higher radiation shield strength at lower energy. A half-value layer (HVL) is another

essential parameter to estimate each safety assembly. It corresponds to the layer thickness, which precisely diminishes half the photon strength of the original. Lower HVL indicates that the thinner thickness of the glass is required to contain half the photon. Herein from Table 4 that the HVL decreases with the increase of Te (see TSH3 sample). The value of HVL at 1.33 MeV is higher than those at the energies of 0.356, 0.662, and 1.173 MeV. For TSH1 glass sample, the HVL values are 1.0112, 1.8249, 2.4436, 2.534 cm at 0.356, 0.662, 1.173 and 1.33 MeV respectively. The lower HVL values of TSH3 with composition 77.53%TeO_2- 7.31%$LiNbO_3$- 4.16%Nb_2O_5- 0.0%TiO_2- 10%BaF_2- 1%La_2O_3 are due to the higher percentage of Te (having higher Z) in this sample, which enhances the possibilities of interaction between gamma photons and absorbing material. The result is also that the higher-density glass has a lower HVL value, which is in agreement with previous research [41– 45]. The Raman spectra for present glasses are shown in Fig. 3. The band of Raman spectra at 441, 500, 665, 650, 741, and 960 cm^{-1}. Also, we not that the Raman bands at the low wavenumber region at 123 and 152 cm^{-1} have not appeared in the present glass which confirmed the intra-molecular asymmetric motion of the Te-O bonds in the glasses network. The band at 441 is due to symmetrical stretching of the $Te_{eq} – O_{ax}$- Te band. The Raman band around 500 cm-1 related to the symmetric vibrations of the Te_2O_2 double bridges [49]. A band around 650 cm^{-1} is due to totally symmetric stretching vibrations of tellurium and axial oxygen ($Te_{-eq} O_{ax}$- Te) in TeO_4 (tbps) trigonal bipyramidal units [49,50] same as the band at 667 cm-1 in the spectrum of pure TeO_2 glass. A band at 741 cm^{-1} can be attributed stretching vibrations of Te-O$^-$ and Te = O bonds containing nonbridging oxygen in TeO_3 tps which strongly appeared in TSH3. A band around 960 cm-1 can be attributed to stretching of Nb and its neighboring NBO in NbO6 octahedra. Finally, the TSH3 glasses have more bridging oxygen (TeO_4) leads to a higher mass attenuation coefficient.
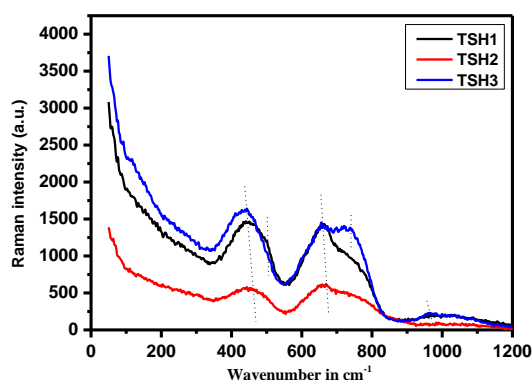
Fig. 3. Raman Spectra of present glasses TSH1, TSH2, and TSH3.

4. Conclusions

In outline, glasses containing different oxides in system 77.53TeO_2-7.31$LiNbO_3$-4.16Nb_2O_5-10% BaF_2-1.0La_2O_3, 71.69TeO_2-7.31$LiNbO_3$-1.0La_2O_3 and 76.69TeO_2-7.31$LiNbO_3$-5TiO_2-10BaF_2-1% La_2O_3 were produced and the software calculated their shielding properties in terms of mass attenuation coefficient, half value layer and mean free path. 76.69TeO_2-7.31$LiNbO_3$-5TiO_2-10BaF_2-1.0 La_2O_3 glasses displayed higher mass attenuation coefficients from the high atomic Te and Ti quantities. The efficiency of shielding of the present glasses was also measured by measuring HVL and MFP values and contrasted to other shielding glasses. On 76.69TeO2-7.31$LiNbO_3$-5TiO_2-10BaF_2-1.0 La_2O_3glasses, the HVL value of present glasses was estimated to improve with increasing photon energy and the lowest values were identified. Based on the results of the present study, it can be established that 76.69TeO_2-7.31$LiNbO_3$-5TiO_2-10BaF2-1.0 La_2O_3 glasses possess good gamma-radiation shielding capability due to higher mass attenuation coefficient values, MFP, bridging oxygen (TeO_4 phase) and lower HVL values.

Acknowledgments

References

[1] H. Nurhafizah, M. Rohani, S. Ghoshal, J. Non-Crystalline Solids **455**, 62 (2017).
[2] A. Abdel-Kader, R. El-Mallawany, M. ElKholy, J. Appl. Phys. **73**(1), 71 (1993).
[3] M. El-Zaidia, A. Ammar, R. El-Mallwany, Phys. Status Solidi A **91**(2), 637 (1985).
[4] H. M. Moawad, H. Jain, R. El-Mallawany, T. Ramadan, M. ElSherbine, J. Am. Ceramic Soc. **85**, 2655 (2002).
[5] I. Z. Hager, R. El-Mallawany, A. Bulou, Phys. B: Condens. Matter **406**, 972 (2011).
[6] R. El-Mallawany, M. Sidkey, H. Afifi, Glass Sci. Technol. **73**, 61 (2000).
[7] C. Yu, Z. Yang, A. Huang, Z. Chai, J. Qiu, Z. Song, D. Zhou, J. Non-Crystalline Solids **457**, 1 (2017).
[8] M. Sidkey, R. El Mallawany, A. Abousehly, Y. Saddeek, Mater. Chem. Phys. **74**(2), 222 (2002).
[9] R. El-Mallawany, M. Sidkey, A. Khafagy, H. Afifi, Mater. Chem. Phys. **37**, 197 (1994).
[10] I. Hager, R. El-Mallawany, J. Mater. Sci. **45**, 897 (2010).
[11] J. Carreaud, A. Labruyere, H. Dardar, F. Moisy, J. R. Duclere, V. Couderc, Opt. Mater. **47**, 99 (2015).
[12] R. El-Mallawany, M. Abdalla, I. Ahmed, Mater. Chem. Phys. **109**(2-3), 291 (2008).
[13] R. El-Mallawany, I. Ahmed, J. Mater. Sci. **43**(16), 5677 (2008).
[14] M. I. Sayyed, S. I. Qashou, Z. Y. Khattari, J. Alloys Compd. **696**, 632 (2017).
[15] M. Sayyed, H. Elhouichet, Radiat. Phys. Chem. **130**, 335 (2017).
[16] K. A. Matori, M. I. Sayyed, H. A. A. Sidek, M. H. M. Zaid, V. P. Singh, J. Non-Crystalline Solids **457**, 97 (2017).
[17] M. I. Sayyed, Can. J. Phys. **94**, 1133 (2016).
[18] M. I. Sayyed, J. Alloys Compd. **688**, 111 (2016).
[19] H. Tekin, E. Kavaz, E. Altunsoy, M. Kamislioglu, O. Kilicoglu, O. Agar, M.Sayyed, N. Tarhan, J. Non-Crystall. Solids **518**, 92 (2019).
[20] M. Dong, X. Xue, Y. Elmahroug, M. Sayyed, M. Zaid, Results Phys. **13**, 102129 (2019).
[21] S. Kaewjaeng, S. Kothan, W. Chaiphaksa, N. Chanthima, R. Rajaramakrishna, H. Kim, J. Kaewkhao, Radiat. Phys. Chem. **160**, 41 (2019).
[22] T. Alharbi, H. F. Mohamed, Y. B. Saddeek, A. Y. El-Haseib, K. S. Shaaban, Radiat. Phys. Chem. **2019**, 108345 (2019).
[23] Z. I. Takai, R. S. Kaundal, M. K. Mustafa, S. Asman, A. Idris, Y. Shehu, J. Mohammad, M. G. Idris, M. Said, Mater. Res. **22**, 1 (2019).
[24] K. M. Kaky, M. Sayyed, F. Laariedh, A. H. Abdalsalam, H. Tekin, S. Baki, Appl. Phys. A **125**(1), 32 (2019).
[25] M. Sayyed, A. Askin, A. M. Ali, A. Kumar, M. Rashad, A. M. Alshehri, M. Singh, J. Non-Crystall. Solids **521**, 119521 (2019).
[26] P. Kaur, K. Singh, M. Kurudirek, S. Thakur, Spectrochim. Acta Part A Mol. Biomol. Spectroscopy **2019**, 117309 (2019).
[27] H. Algrani, M. Reben, E. Yousef, Optik **156**, 720 (2018).
[28] A. W. El-Sayed, M. A. Bourham, Ann. Nucl. Energy **85**, 306 (2015).
[29] L. Gerward, N. Guilbert, K. B. Jensen, H. Levring, Radiat. Phys. Chem. **71**, 653 (2004).
[30] S. Y. El-Kameesy, S. Abd El-Ghany, M. A. Azooz, Y. A. El-Gammam, W. J. Condens. Matt. Phys. **3**, 198 (2013).
[31] K. A. Mahmoud, M. I. Sayyed, O. L. Tashlykov, Nucl. Eng. Technol. **51**, 1835 (2019).
[32] M. Al-Buriahi, Y. Rammah, Appl. Phys. A **125**(10), 678 (2019).
[33] H. Tekin, E. Kavaz, E. Altunsoy, O. Kilicoglu, O. Agar, T. Erguzel, M. Sayyed, Ceram. Int.

45(8), 9934 (2019).

[34] E. Kavaz, H. Tekin, O. Agar, E. Altunsoy, O. Kilicoglu, M. Kamislioglu, M. Abuzaid, M. Sayyed, Ceram. Int. **45**(12), 15348 (2019).

[35] O. Kilicoglu, H. O. Tekin, V. P. Singh, Eur. J. Sci. Technol. **173**(15), 591 (2019).

[36] El-Sayed A. Waly, Ghada Shkoukani Al-Qous, Mohamed A. Bourham, Radiat. Phys. Chem. **150**, 120 (2018).

[37] Y. Al-Hadeethi, M.I. Sayyed, Ceramics International **46**, 4795 (2020).

[38] SCHOTT.http://www.schott.com/advanced_optics/english/products/opticalmaterials/ special-materials/radiation-shielding-glasses/index.html. (accesed 03.09. 2018) 2018.

[39] A. Aşkın, M. I. Sayyed, Amandeep Sharma, M. Dal, R. El-Mallawany, M. R. Kaçal, Journal of Non-Crystalline Solids **521**, 119489 (2019).

[40] R. El-Mallawany, A. Abd El-Moneim, Phys. Status Solidi A **166**(2), 829 (1998).

[41] A. Kumar, Radiat. Phys. Chem. **136**, 50 (2017).

[42] S. Kaewjaeng, S. Kothan, N. Chanthima, H.J. Kim, J. Kaewkhao, Materials Today: Proceedings **5**, 14901 (2018).

[43] M. Kurudirek, J. Alloy.Compd. **727**, 1227 (2017).

[44] M. I. Sayyed, Alloys Compd. **695**, 3191 (2017).

[45] K. Singh et al., Nucl. Instrum. Methods Phys. Res. Sect. B **266**(6), 944 (2008).

[46] B. Speit, Radiation-shielding Glasses Providing Safety Against Electrical Discharge and Being Resistant to Discoloration, 1991 Google Patents.

[47] I. I. Bashter, Ann. Nucl. Energy **24**(17), 1389 (1997).

[48] V. Kamalaker, G. Upender, Ch. Ramesh, V. Chandra Mouli, Spectrochimica Acta Part A **89**, 149 (2012).

[49] G. Upender, S. Ramesh, M. Prasad, V. G. Sathe, V. C. Mouli, Journal of Alloys and Compounds **504**, 468 (2010).